Letters

Multielement Resonant Converters With a Notch Filter on Secondary Side

Hongfei Wu, *Member, IEEE*, Xiang Jin, Haibing Hu, and Yan Xing, *Member, IEEE*

***Abstract*—This letter proposes novel multielement resonant converters, which are improved topologies of the conventional *LLC* resonant converter, for voltage step-up applications. A notch filter is introduced into the secondary side of the *LLC* resonant converter. The voltage gain of the proposed resonant converters can be as low as zero with limited switching frequency range. Therefore, the start-up and short output circuit protection issues of the conventional *LLC* resonant converter can be solved with the proposed solutions. Furthermore, the circulating energy of the resonant tank can be reduced as well. In comparison with the multielement resonant converters with a notch filter on primary side, the proposed converter can help to reduce the conduction losses associated with the notch filter and provide higher voltage gain at the resonant frequency. The topologies and characteristics of the proposed resonant converters are analyzed. Experimental results are given to verify the effectiveness and the advantages of the proposed solutions.**

***Index Terms*—DC–DC converter, *LLC* resonant converter, multiresonant, notch filter.**

I. Introduction

LLC resonant converter is gaining much more attention than ever before and has been applied in several applications, such as power supplies for servers [1], front-end converters for renewable power systems [2], and battery chargers for electrical vehicles [3]. The most attractive characteristics of the *LLC* resonant converter are excellent soft switching performance, improved efficiency, reduced electromagnetic interference, and voltage step-up capability.

However, the *LLC* resonant converter still has some issues to be solved. The overcurrent protection is required within the entire operation conditions, especially for the start-up and overload conditions. Since the voltage gain curve of the conventional *LLC* resonant converter is relatively flat when the switching frequency f_s is higher than the resonant frequency f_r of the resonant tank, high voltage and current stress will occur at the start-up moment if the start-up switching frequency is not high enough [4]. Such a high switching frequency is not achievable usually. Even though high switching frequency can be achieved, large voltage and current stress can still happen if the switching frequency decreases too quickly [5]. To solve the start-up and overcurrent protection issues, optimal trajectory control strategies are proposed in [5] and [6]. These strategies are effective for start-up but difficult to implement, meanwhile, the overload protection issue cannot be solved. Increased conduction losses due to circulating energy generation is an another issue of the *LLC* resonant converter. The transferred power of the *LLC* resonant converter is controlled by a square-wave voltage inverter and a resonant network in a piecewise sinusoidal manner. As a result, only the fundamental power is transferred to the output and the high-order harmonics of input voltage and current of the resonant tank exhibit reactive power, which does not contribute to the power delivery. Therefore, the power processed by the resonant converter is usually larger than that of a pulse width modulation (PWM) converter with the same output power [7]. Fortunately, these issues are solved perfectly by introducing a notch filter into the primary side of the conventional *LLC* resonant converter [7]–[10]. As shown in Fig. 1, the notch filter is placed on the primary side, the input side is a half-bridge (HB) or full-Bridge (FB) inverter, while the output side can be FB or center-tapped (CT) rectifier in [7]–[10]. However, the additional conduction losses introduced by the notch filter will decrease the efficiency significantly, especially when the converter is applied to large input current with low-input voltage applications, such as the front-end converters for renewable power systems. It is because all the currents, including the load current and magnetizing current associated with L_m flow through the notch filter.

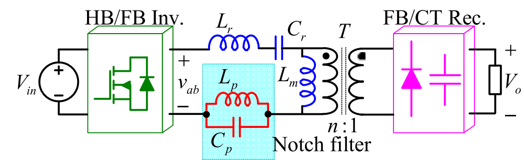

Fig. 1. Structure of the *LLC* resonant converter with a notch filter on primary side.

To solve these issues, an improved *LLC* resonant converter with a notch filter on the secondary side is proposed for the voltage step-up applications. The start-up and overcurrent protection issues can be solved perfectly because the voltage gain of the converter can be as low as zero. The circulating energy and conduction losses are reduced because higher harmonics are utilized to deliver power, while only low current on the secondary high-voltage side flows through the notch filter. Furthermore,

Manuscript received October 13, 2015; revised November 20, 2015; accepted December 5, 2015. Date of publication December 9, 2015; date of current version January 7, 2016. This work was supported in part by the National Natural Science Foundation of China under Grant 51407092, in part by the Natural Science Foundation of Jiangsu Province, China under Grant BK20140812, and in part by the Jiangsu province university outstanding science and technology innovation team project.

The authors are with the Jiangsu Key Laboratory of New Energy Generation and Power Conversion, College of Automation Engineering, Nanjing University of Aeronautics and Astronautics, Nanjing 210016, China (e-mail: wuhongfei@nuaa.edu.cn; jxiang@nuaa.edu.cn; huhaibing@nuaa.edu.cn; xingyan@nuaa.edu).

Color versions of one or more of the figures in this paper are available online at http://ieeexplore.ieee.org.

Digital Object Identifier 10.1109/TPEL.2015.2507263

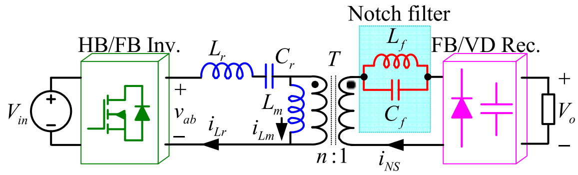

Fig. 2. Structure of the proposed *LLC–LC* multiresonant converter.

higher voltage gain at the resonant frequency can be obtained with the proposed converter.

II. Circuit Construction and Operation Principle

The structure of the proposed *LLC--LC* multiresonant converter is shown in Fig. 2, where an *LLC* resonant tank composed of L_r, C_r, and L_m is employed on the primary side, while a notch filter composed of L_f and C_f is employed on the secondary side. The input side of the converter can be HB, FB, or a three-level inverter, and the output side can be FB or voltage-doubler (VD) rectifier. It should be noted that the CT rectifier cannot be used. In comparison with the *LLC* resonant converter with a notch filter on primary side, as shown in Fig. 1, the proposed converter is more suitable for high-output voltage applications. Since, the notch filter is placed on the secondary side, the resonant current associated the magnetizing inductor L_m will not flow through the notch filter, which is benefit for reducing the current stresses and conduction losses of the notch filter.

Similar to the multiresonant converter in [7]–[10], four resonant frequencies, f_{r0}–f_{r3}, can be obtained as well with the proposed *LLC–LC* multiresonant converter. These resonant frequencies are given as follows:

$$f_{r0} = \frac{1}{2\pi\sqrt{(L_r + L_m)C_r}} \tag{1}$$

$$f_{r1} = \sqrt{\frac{1 + A + B - \sqrt{(1 + A + B)^2 - 4B}}{2B}} \cdot f_r \tag{2}$$

$$f_{r2} = \frac{1}{2\pi\sqrt{L_f C_f}} \tag{3}$$

$$f_{r3} = \sqrt{\frac{1 + A + B + \sqrt{(1 + A + B)^2 - 4B}}{2B}} \cdot f_r. \tag{4}$$

In (2) and (4), *A*, *B*, and f_r are defined as

$$A = \frac{n^2 L_f L_m}{n^2 L_f L_r + L_m L_r} \tag{5}$$

$$B = \frac{C_f L_f L_m}{C_r (n^2 L_p L_r + L_m L_r)} \tag{6}$$

$$f_r = \frac{1}{2\pi\sqrt{L_r C_r}} \tag{7}$$

where *n* is the primary-to-secondary turns ratio of the transformer *T*. Conceptually, the resonant frequency f_{r1} functions as the role of the traditional *LLC* resonant converter. It helps to deliver the fundamental component to the load. The resonant frequency f_{r2}, which is the parallel resonant frequency of the notch filter, can provide an infinite impedance and create zero voltage gain for the converter. As a result, the current can be limited inherently at this switching frequency if overload or even shorted output condition occurs. The resonant frequency f_{r3} provides very low impedance for the higher order harmonics. Conceptually, f_{r3} enhances the power delivery with the injection of higher order harmonics. Therefore, f_{r3} can help to reduce the reactive power and conduction losses of the resonant tank, which is the same as the *LLC* resonant converter with a notch filter on primary side [7]–[10].

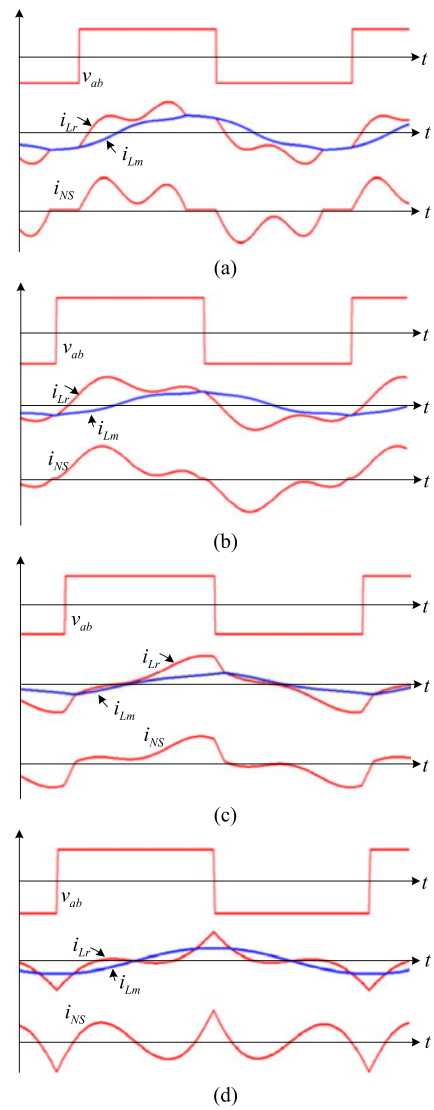

Fig. 3. Simulated operation waveforms of the *LLC–LC* resonant converter, (a) $f_s < f_{r1}$, (b) $f_s = f_{r1}$, (c) $f_s > f_{r1}$, (d) $f_s = f_{r2}$, and short output.

The operation principles and waveforms of the proposed *LLC–LC* resonant converter is similar to the multiresonant converter in [7]–[10]. Frequency modulation can be adopted to regulate the output. The preferred switching frequency f_s range is $f_s \leq f_{r1}$, in which case zero-voltage-switching (ZVS) and zero-current-switching (ZCS) can be achieved for the primary side

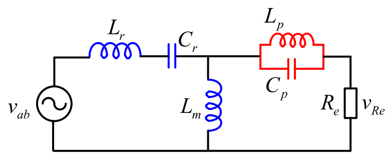

Fig. 4. Simplified circuit of the proposed *LLC–LC* resonant converter.

active switches and the secondary side diodes, respectively. The maximum switching frequency $f_{s\max}$ is recommended to f_{r2}. When $f_{r1} < f_s < f_{r2}$, ZVS can be achieved for the primary-side switches, but ZCS will be lost for the secondary-side diodes. The soft-switching performance can be verified by the simulated operation waveforms of the proposed converter, as shown in Fig. 3. From Fig. 3, it can be seen that higher order harmonics have been injected to the waveforms of i_{Lr} and i_{NS}, which can help to enhance the power delivery. From Fig. 3(d), it can be seen that, when $f_s = f_{r2}$ and the output short circuit occurs, the current in the resonant tank is limited.

III. Characteristics and Analysis

A. Characteristics

The proposed *LLC–LC* multiresonant converter can be simplified to the one shown in Fig. 4, where R_e is the equivalent load resistor, and

$$L_p = n^2 L_f \tag{8}$$

$$C_p = \frac{C_f}{n^2}. \tag{9}$$

To simplify the analysis, the resonant inductor ratio k_{Lp} and k_{Ln}, resonant capacitor ratio k_C, and quality factor Q are defined as follows:

$$k_{\mathrm{Lp}} = \frac{L_p}{L_r} \tag{10}$$

$$k_{\mathrm{Ln}} = \frac{L_r}{L_m} \tag{11}$$

$$k_C = \frac{C_p}{C_r} \tag{12}$$

$$Q = \frac{\sqrt{L_r/C_r}}{R_e}. \tag{13}$$

According to Fig. 4, the normalized voltage gain M of the resonant tank can be derived and given as follows:

$$M(Q, f_n) = \left| \frac{1}{1 + \frac{jk_{Lp} Q g_{f1} f_n}{1 - k_{Lp} k_C (f_n g_{f1})^2}} \times \frac{1}{1 + k_{Ln}\left[1 - \frac{1}{(f_n g_{f1})^2}\right] + \frac{jQ(1 - k_{Lp} k_C f_n^2 g_{f1}^2)}{1 - k_{Lp} k_C f_n^2 g_{f1}^2 + jQ k_{Lp} f_n g_{f1}}\left(g_{f1} f_n - \frac{1}{g_{f1} f_n}\right)} \right| \tag{14}$$

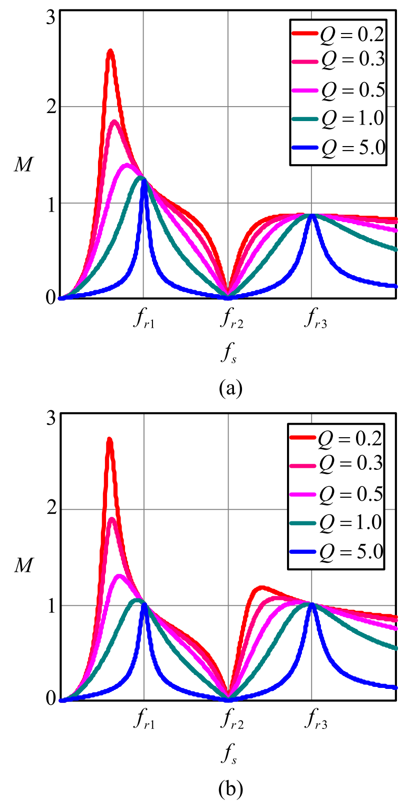

Fig. 5. Normalized voltage gain curves of the resonant tank, (a) the proposed converter, (b) *LLC* resonant converter with notch filter on primary side.

where

$$g_{f1} = \sqrt{\frac{1 + A + B - \sqrt{(1 + A + B)^2 - 4B}}{2B}} \tag{15}$$

$$f_n = \frac{f_s}{f_{r1}}. \tag{16}$$

Substituting f_{r1}, f_{r2}, and f_{r3} into (14), the voltage gain at the three resonant frequencies is derived as

$$\begin{cases} M(Q, f_{r1}) = \dfrac{1}{1 + k_{Ln}\left(1 - \dfrac{1}{g_{f1}^2}\right)} \\ M(Q, f_{r2}) = 0 \\ M(Q, f_{r3}) = \dfrac{1}{1 + k_{Ln}\left(1 - \dfrac{f^2{}_{r1}}{f^2{}_{r3} g_{f1}^2}\right)}. \end{cases} \tag{17}$$

It can be seen that the constant voltage gains, which are independent on the load, can be obtained at the three resonant frequencies. According to (15), (5), and (6), one can find that 0 $< g_{f1} <$1 is always satisfied.

Therefore, the voltage gain at f_{r1} is always greater than one, while voltage gain at f_{r2} is always lower than one. The voltage gain curves of the proposed converter with $k_{Lp} = 0.85$, $k_{Ln} =$ 0.2, and $k_C = 0.57$ are illustrated in Fig. 5(a). As a comparison, the voltage gain curves of the *LLC* resonant converter with a notch filter on primary side and the same k_{Lp}, k_{Ln}, and k_C

are plotted in Fig. 5(b) according to the analysis in [7] and [10]. It can be seen that both the two converters can provide infinite impedance and zero voltage gain at f_{r2}, which can help to achieve soft-start, overload, and inherent inrush current protection. When the notch filter is placed on the secondary side, higher voltage gain can be achieved at the resonant frequency f_{r1}, which can help to reduce the turns ratio of the transformer. Meanwhile, the circulating current associated with L_m will not flow through the notch filter, which is benefit for reducing the conduction losses. However, it should be noted that the voltage gain of the presented *LLC–LC* converter at f_{r3} is slightly lower than that with the notch filter on the primary side.

B. Design Considerations

The analysis and experimental results in [9] and [10] indicate that the voltage gain characteristics of the modified *LLC* resonant converter with a notch filter is almost the same as the conventional *LLC* resonant converter, when the operation frequency f_s is lower than the resonant frequency f_{r1}. Meanwhile, $f_s < f_{r1}$ is the preferred operation region for normal operation of the resonant converter from the view of the soft-switching performance. Therefore, the parameters of L_r, C_r, and L_m of the proposed *LLC–LC* resonant converter can be designed by using the design method of the conventional *LLC* resonant converter according to the requirement of the normal operation.

The excitation voltage $v_{\rm ab}$ of the resonant tank is a square waveform voltage source. According to the Fourier analysis,

$$v_{\rm ab} = \frac{4}{\pi} V_{\rm AB} \sum_{n=1,3\ldots}^{\infty} \frac{\sin(n\omega_s t)}{n} \tag{18}$$

where $V_{\rm AB}$ and ω_s are the peak-to-peak value and the angular frequency of $v_{\rm ab}$, respectively. For the conventional *LLC* resonant converter, only the fundamental component of $v_{\rm ab}$ contributes to power delivery and the high-order harmonics exhibit reactive power. By introducing a notch-filter, high-order current harmonics can be injected to the resonant tank and used to deliver power. As a result, the reactive power and conduction loss can be reduced. Therefore, the resonant frequency f_{r3}, which provides low impedance for the higher order harmonics is recommended to be designed three times of f_{r1}. In this case, the third harmonics can be utilized. However, it should be noted that, with variable frequency operation, the third harmonics injection will become weak once the switching frequency is far away from f_{r1}. Therefore, conceptually, the modified multielement resonant converter is not suitable for wide frequency variation applications, no matter the notch filter is placed on primary side or secondary side.The main function of the notch filter is to provide excellent voltage regulation ability for the *LLC* resonant converter. The resonant frequency f_{r2} of the notch filter is designed to achieve the overload protection and soft start. According to Fig. 5, f_{r2} is in the range of [f_{r1}, f_{r3}]. To avoid the notch filter affecting the power transfer of fundamental and third harmonics, f_{r2} should be not too close to f_{r1} and f_{r3}. On the other hand, to reduce the size, volume, and power loss of the notch filter, f_{r2} should be designed as high as possible. In practice, $1.5f_{r1} \leq f_{r2} \leq 2.5f_{r1}$ is recommended.

TABLE I
PERFORMANCE COMPARISON

Location of the notch filter	Primary side	Secondary Side
Normalized current stress	High	Low (only load current)
Voltage gain at f_{r1}	1	>1
Third current harmonic injection	Good	Poor
Voltage gain range corresponding to $f_s < f_{r1}$	Good (the same as conventional *LLC*)	Poor
Preferred applications	Voltage step-down with low current on primary side	Voltage step-up with low current on secondary

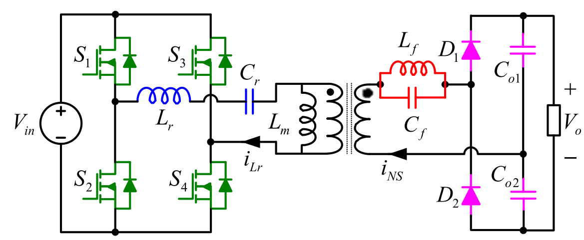

Fig. 6. Topology of the proposed *LLC–LC* multiresonant converter with VD rectifier.

C. Performance Comparison

To help design tradeoff and topology selection in engineering applications, the comparison between different locations of notch filter in the *LLC* resonant converter is listed in Table I. It can be seen that although the current stress and conduction loss associated with the magnetizing inductor L_m is avoided by placing the notch filter on secondary side, the third harmonic injection capability of the presented converter is lower. The voltage gain at f_{r1} is improved, but the voltage gain range with $f_s < f_{r1}$ is narrowed. It is obvious that each converter has its advantages and disadvantages.

IV. EXPERIMENTAL VERIFICATION

To verify the effectiveness of the proposed *LLC–LC* resonant converter, a full-bridge converter with VD rectifier, as shown in Fig. 6, is built and tested. The converter is designed for a PV-sourced renewable power system. The maxim open-circuit voltage of the input source is 50 V, while the maximum power point tracking voltage range is 25–40 V. Output voltage $V_{\rm o} =$ 400 V and rated output power $P_{\rm o} =$ 400 W. L_m and L_r is designed to be 8.1 and 2.17 uH, respectively, according to ZVS conditions and the voltage gain requirement. f_{r1} is chosen as 120 kHz, and f_{r2} and f_{r3} are chosen to be 2.5 times and 3 times of f_{r1}, respectively. Based on (1)–(7), $L_f =$ 14.5 uH and C_f $=$ 20 nF are obtained. Meanwhile, according to (17), the normalized voltage gain at f_{r1} is 1.1. Therefore, the transformer turns ratio $n =$ 1:4.5 (turns of primary and secondary windings are 6 and 27, respectively). In this case, the optimized operation frequency f_{r1} is corresponding to $V_{\rm in} =$ 40 V. The normalized voltage gain curves of the converter with the above parameters are illustrated in Fig. 5(a). The switches and diodes are as follows: S_1–S_4: IPP093N06N3, D_1 and D_2: STTH5L06.

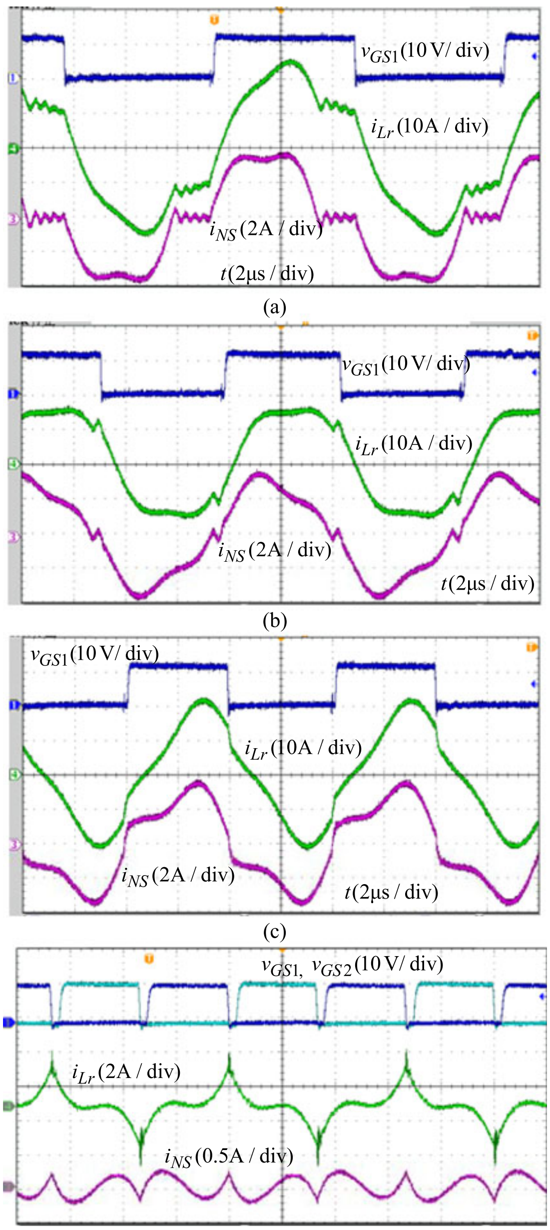

Fig. 7. Steady-state waveforms under full-load, (a) $V_{\rm in} = 30$ V with $f_s < f_{r1}$, (b) $V_{\rm in} = 40$ V with $f_s = f_{r1}$, (c) $V_{\rm in} = 45$ V with $f_s > f_{r1}$, (d) output short circuit and $f_s = f_{r2}$.

The steady-state switching waveforms of the proposed *LLC–LC* multiresonant converter with full-load output are shown in Fig. 7, where $v_{\rm GS1}$ and $v_{\rm GS2}$ are the driving voltages of the primary-side switches S_1 and S_2, $i_{\rm Lr}$, and $i_{\rm NS}$ are the currents flow through resonant inductor L_r and the secondary winding of transformer, respectively. Fig. 8(a) is the waveforms when $V_{\rm in} = 30$ V and the switching frequency $f_s < f_{r1}$, Fig. 7(b) is the waveforms when $V_{\rm in} = 40$ V and $f_s = f_{r1}$, Fig. 7(c) is the waveforms when $V_{\rm in} = 45$ V and $f_s > f_{r1}$, while Fig. 7(d) is the waveforms when output short circuit and $f_s = f_{r2}$. It can be seen that the operation waveforms of the proposed converter is similar to the *LLC* resonant converter with a notch filter on the primary side [7]–[10]. The current circulating in the resonant tank when output short circuit occurs is very small. The experimental waveforms are consistent with the simulated results shown in Fig. 3 pretty well.

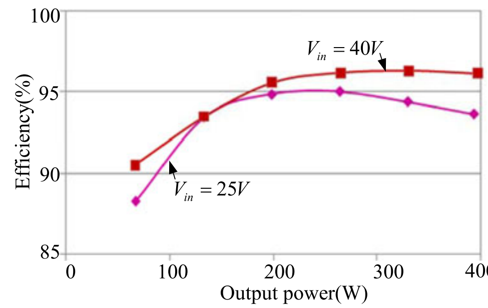

Fig. 8. Efficiency of the proposed *LLC–LC* resonant converter.

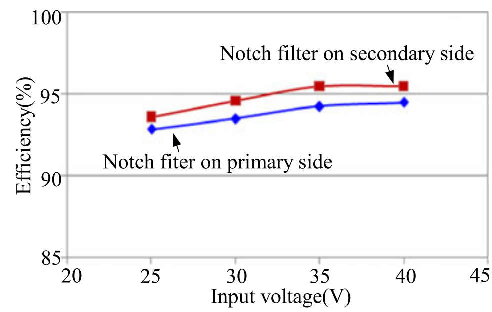

Fig. 9. Efficiency comparison under full-load.

The efficiency curves of the proposed converter under different input voltages are shown in Fig. 8. It can be seen that the trend of the efficiency curves is similar to that of the conventional *LLC* resonant converter. Higher efficiency can be achieved at the resonant frequency f_{r1}, while the efficiency decreases as the input voltage decreases.

To evaluate the efficiency improvement of the proposed multiresonant converter, another prototype based on the *LLC* resonant converter with a notch filter on the primary side is built as well. In addition to the position of the notch filter, the topology of the converter is the same as the one shown in Fig. 6. To make a fair comparison, the resonant frequencies f_{r1}, f_{r2}, and f_{r3} of this prototype is the same as that of the proposed converter. However, it should be noted that, as indicated by Fig. 5, the normalized voltage gain at f_{r1} is 1.0 when the notch filter is placed on the primary side. Therefore, to achieve the same voltage step-up ratio at the resonant frequency f_{r1} (with $V_{\rm in} =$ 40 V), the transformer's turns ratio is designed to be 1:5 (turns of primary and secondary windings are 6 and 30, respectively) when the notch filter is placed on the primary side. Therefore, three turns are reduced for the secondary winding by placing the notch filter on the secondary side. The efficiency curves with full-load output are shown in Fig. 9. It can be seen that higher conversion efficiency is achieved by placing the notch filter on the secondary side due to the reduced conduction losses.

V. Conclusion

An improved multiresonant converter has been proposed in this letter. In comparison with the *LLC* resonant converter with a notch filter on primary side, lower RMS current and lower conduction losses can be achieved because only the load current flows through the notch filter. In addition, the voltage gain can be as low as zero when the converter operates at the parallel resonant frequency of the notch filter, which is the same as the *LLC* resonant converter with a notch filter on the primary side. Furthermore, higher voltage gain is achieved at the resonant frequency, which can help to decrease the turns ratio of the transformer and increase the efficiency. These features make the proposed multiresonant converter more suitable for applications with low-input and high-output voltages, such as the front end converters for renewable power systems. Experimental results on a full-bridge resonant converter with VD rectifier are provided to verify the effectiveness of the proposed multiresonant converter.

References

[1] H. Nguyen, R. Zane, and D. Maksimovic, "ON/OFF control of a modular DC-DC converter based on active-clamp LLC modules," *IEEE Trans. Power Electron.*, vol. 30, no. 7, pp. 3748–3760, Jul. 2015.

[2] Q. Zhang, C. Hu, L. Chen, A. Amirahmadi, N. Kutkut, Z. J. Shen, and I. Batarseh, "A center point iteration MPPT method with application on the frequency-modulated LLC mocroinverter," *IEEE Trans. Power Electron.*, vol. 29, no. 3, pp. 1262–1274, Mar. 2014.

[3] H. Haga and F. Kurokawa, "A novel modulation method of the full bridge three-level LLC resonant converter for battery charger of electrical vehicles," in *Proc. IEEE Energy Convers. Congr. Expo.*, 2015, pp. 5498–5504.

[4] (2006, Feb.). On Semiconductor NCP1395LLCGEVB: 240W LLC evaluation board [Online]. Available: http://www.onsemi.com/PowerSolutions/evalBoard.do?id=NCP1395LLCGEVB

[5] W. Feng and F. C. Lee, "Optimal trajectory control of LLC resonant converters for soft start-up," *IEEE Trans. Power Electron.*, vol. 29, no. 3, pp. 1461–1468, Mar. 2014.

[6] R. Zheng, B. Liu, and S. Duan, "Analysis and parameter optimization of start-up process for LLC resonant converter," *IEEE Trans. Power Electron.*, vol. 30, no. 12, pp. 7113–7122, Dec. 2015.

[7] D. Fu, F. C. Lee, Y. Liu, and M. Xu, "Novel Multi-element resonant converters for front-end DC/DC converters," in *Proc. IEEE Power Electron. Spec. Conf.*, 2008, pp. 358–364.

[8] D. Huang, P. Kong, F. C. Lee, and D. Fu, "A novel integrated multi-elements resonant converter," in *Proc. IEEE Energy Convers. Congr. Expo.*, 2011, pp. 3808–3815.

[9] T. Mishima, H. Mizutani, and M. Nakaoka, "An LLC resonant full-bridge inverter-lin DC-DC converter with an anti-resonant circuit for practical voltage step-up/down regulation," in *Proc. IEEE Energy Convers. Congr. Expo.*, 2012, pp. 3533–3540.

[10] H. Mizutani, T. Mishima, and M. Nakaoka, "A dual pulse modulated five-element multi-resonant DC-DC converter and its performance evaluations," in *Proc. IEEE Energy Convers. Congr. Expo.*, 2013, pp. 4912–4919.